

REPORT DOCUMENTATION PAGE

Form Approved
OMB No. 0704-0188

Public reporting burden for this collection of information is estimated to average 1 hour per response, including the time for reviewing instructions, searching existing data sources, gathering and maintaining the data needed, and completing and reviewing this collection of information. Send comments regarding this burden estimate or any other aspect of this collection of information, including suggestions for reducing this burden to Department of Defense, Washington Headquarters Services, Directorate for Information Operations and Reports (0704-0188), 1215 Jefferson Davis Highway, Suite 1204, Arlington, VA 22202-4302. Respondents should be aware that notwithstanding any other provision of law, no person shall be subject to any penalty for failing to comply with a collection of information if it does not display a currently valid OMB control number. PLEASE DO NOT RETURN YOUR FORM TO THE ABOVE ADDRESS.

| | | | | | |
|--|------------------|-------------------------|---------------------------------------|--|---|
| 1. REPORT DATE (DD-MM-YYYY) 16/02/2003 | | 2. REPORT TYPE Final | | 3. DATES COVERED (From - To) 16/09/2002 to 16/02/2003 | |
| 4. TITLE AND SUBTITLE PHASE I OPTION PROGRAM FINAL REPORT EMBEDDED SENSOR TECHNOLOGY FOR SRM HEALTH MONITORING MONITORING | | | | 5a. CONTRACT NUMBER DAAH01-02-R099 | |
| | | | | 5b. GRANT NUMBER A012-770 | |
| | | | | 5c. PROGRAM ELEMENT NUMBER | |
| | | | | 5d. PROJECT NUMBER A01-166 | |
| 6. AUTHOR(S) HERBERT CHELNER | | | | 5e. TASK NUMBER | |
| | | | | 5f. WORK UNIT NUMBER | |
| | | | | | |
| 7. PERFORMING ORGANIZATION NAME(S) AND ADDRESS(ES) MICRON INSTRUMENTS 4509 RUNWAY St SIMI VALLEY, CA 93063 | | | | 8. PERFORMING ORGANIZATION REPORT NUMBER 02-221B | |
| 9. SPONSORING / MONITORING AGENCY NAME(S) AND ADDRESS(ES) US ARMY AVIATION AND MISSILE MSAM-RD-PS-S REDSTONE ARSENAL, AL 35898-5000 | | | | 10. SPONSOR/MONITOR'S ACRONYM(S) AMCOM | |
| | | | | 11. SPONSOR/MONITOR'S REPORT NUMBER(S) | |
| 12. DISTRIBUTION / AVAILABILITY STATEMENT APPROVED FOR PUBLIC RELEASE: DISTRIBUTION UNLIMITED | | | | | |
| 13. SUPPLEMENTARY NOTES | | | | | |
| 14. ABSTRACT Report developed under SBIR contract for topic A01-166 'Embedded Sensor Technology for Solid Rocket Motor Health Monitoring'. This report presents the progress achieved during this Phase I Option Program period. Results from constant load tests indicate that the current build standard of sensor is stable and shows little creep when under 75% full-scale tensile load for over a year. The sample broke at the bond line after 55 weeks and the sensor zero changed by only 3.8 psi with no change in the sensitivity. All required sensors have been manufactured and delivered with full specification and calibration sheets. The development of the Precision Semiconductor Strain Gage Matching System is reported and the expected improvement in performance confirmed. | | | | | |
| 15. SUBJECT TERMS SOLID ROCKET MOTORS (SRM), EMBEDDED SENSORS, HEALTH MONITORING, MICROELECTROMECHANICAL (MEMS) | | | | | |
| 16. SECURITY CLASSIFICATION OF: | | | 17. LIMITATION OF ABSTRACT SAR | 18. NUMBER OF PAGES 12 | 19a. NAME OF RESPONSIBLE PERSON HERBERT CHELNER |
| a. REPORT U | b. ABSTRACT U | c. THIS PAGE U | | | 19b. TELEPHONE NUMBER (include area code) (805) 522 4676 |

20030321 110

PHASE I SMALL BUSINESS INNOVATION RESEARCH (SBIR) PROGRAM

Proposal No: A012-0770

Topic No: A01-166

Start Date: 1/31/2002

Finish Date: 2/16/2003

Firm Name: Micron Instruments

Mail Address: 4509 Runway St, Simi Valley, CA 93063

Principal Investigator: Mr Herb Chelner

**PHASE I OPTION PROGRAM
FINAL REPORT
PERIOD 9/16/2002 TO 2/16/2003**

**EMBEDDED SENSOR TECHNOLOGY FOR SOLID ROCKET
MOTOR HEALTH MONITORING**

MICRON REPORT NO: 02-221B


ABSTRACT

Report developed under SBIR contract for topic A01-166 'Embedded Sensor Technology for Solid Rocket Motor Health Monitoring'. This report presents the progress achieved during this Phase I Option Program period. Results from constant load tests indicate that the current build standard of sensor is stable and shows little creep when under 75% full-scale tensile load for over a year. The sample broke at the bond line after 55 weeks and the sensor zero changed by only 3.8 psi with no change in the sensitivity. All required sensors have been manufactured and delivered with full specification and calibration sheets. The development of the Precision Semiconductor Strain Gage Matching System is reported and the expected improvement in performance confirmed.

DECLARATION OF TECHNICAL DATA CONFORMITY

The Contractor, Micron Instruments, hereby declares that, to the best of its knowledge and belief, the technical data delivered herewith under Contract No DAAHo1-02-C-R099 is complete, accurate, and complies with all requirements of the contract.

Date: 16th February, 2003.



Herbert Chelner, President

CONTENTS

| | page |
|--|------|
| SECTION 1 Precision Matching System (PMS) | 3 |
| 1.1 Typical Semiconductor Gage Matching System and Limitations | 3 |
| 1.2 PMS Description and Operation | 3 |
| 1.3 Discussion of Results | 5 |
| 1.4 Conclusions | 7 |
| SECTION 2 Long Term Measurement Stability | 7 |
| SECTION 3 Conclusions and Recommendations | 9 |

SECTION 1 –Precision Matching System (PMS)

1.1 Typical Semiconductor Gage Matching System and Limitations

Manufacturers of semiconductor gages sell their gages in thermally matched sets of two or four. Unlike foil or wire gages, the semiconductor gage has a very large change in resistance with temperature. If not thermally matched for slope and intercept, temperature compensation for balance would be difficult and performance would be compromised.

For thermal testing gages are normally installed (soldered) free standing on circuit boards so that induced stress is minimized. The circuit board is designed to go into a temperature chamber. Air that is heated or cooled enters the chamber from one side and exits at the opposite side. Small temperature chambers are used to minimize the thermal differential across the chamber, which determines the resistance tolerance in the gage matching. Approximately fifty gages are installed onto a circuit board and four boards are inserted and form a three dimensional array in the center of the chamber. The object is to minimize the thermal differential across the chamber.

To read the gage resistance, power is applied from a constant current supply and the circuit compensates for any line change. A computer measures the gage resistance taking multiple readings over a finite period of time and averages them. This is done to reduce noise error and increase the accuracy. Resistive readings are taken at -50, 0, 78 and 278 °F. The gage sets are matched within plus or minus two ohms. Due to the thermal differentials across the three dimensional array of circuit boards, thermal resistive errors of up to +/- four percent of the ambient resistance is possible. These resistive errors increase the thermal non-linearity and decrease the long-term stability when used in bridges for sensor application.

1.2 PMS Description and Operation

The circuit board contains 48 gages and consists of two rows of 27 evenly spaced measurement positions. Each row has a Resistive Temperature Device (RTD) in (slot 1) to measure temperature at the beginning of the row, twelve gages and a middle RTD in (slot 14) in the center of the row. This is referred to as a quad. The center RTD is followed by twelve more gages and the rear RTD is slot 27 and is referred to as quad two. The other side of the circuit board is the same and called quads three and four. Only the gages have position numbers. Quad one is 1 through 12, quad 2 positions 13 through 24, quad 3 positions 25 through 36 and through quad 16 with positions 181 through 192. A populated circuit board, one of four, is shown in Figure 1 and the arrangement in the oven is shown in Figure 2.

On each circuit board, in one unique position, is a known precision resistor. This resistor is a check on the accuracy of the system and allows the computer to locate the particular circuit board in any position of the test array. The temperature of each position between the RTDs bracketing the gages in one slot is calculated using $Y = mX + B$. Assume the temperature changes linearly. The computer communicates with the temperature chamber and starts with a command to set 78 ° F, rest for one hour and take data. The front RTD takes 17 samples at one milli- second per sample and averages the data. This approximates one cycle of a 60 Hz signal and should eliminate 60 Hz noise. The voltage to the RTD is monitored and its precision data and RTD correction formulas are in memory to determine temperature vs. resistance to 0.01 ° F. Each gage and the middle RTD are sampled in the same way. Using the Tc slope of each gage

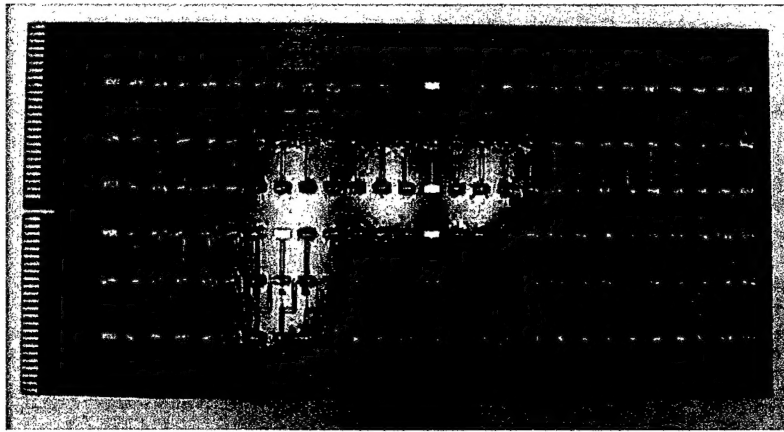


Figure 1. Populated Circuit Board

and the straight line vs. position change in temperature, the resistance of each gage is corrected to 78 ° F. The number crunching is done after the actual data taking approximately one half second per quad and eight seconds to take the entire array of data. The data at 78 ° F was accurate and repeatable. Data taken at 0 ° F was not repeatable and the worst errors were seen at 278 F. Analysis showed that the temperature chamber hot and cold air turbulence with the fan on and the chamber heaters or CO2 relays cycling on and off was causing a significant problem. The mass of the RTD's although very small was two orders of magnitude greater than the gages and there was too great a phase difference.

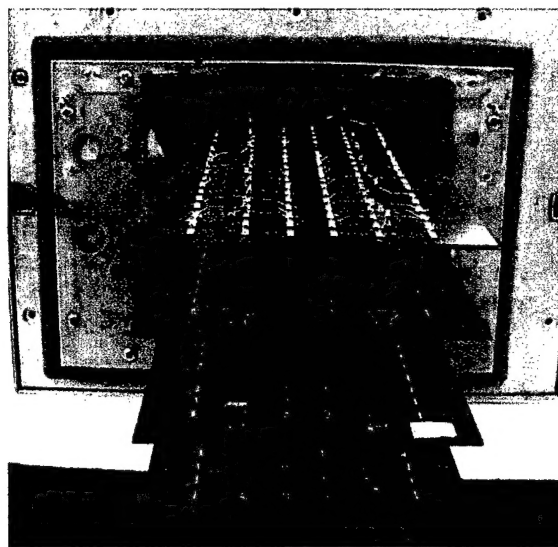


Figure 2. Circuit Boards in Oven

A digital software long-term noise filter was designed. Each 17-second sample average will be a data point. At 278 ° F, forty data points will be taken and averaged which is called the floating long term average (FLTA). The forty-first data point will be algebraically compared to the FLTA and if less than 0.10 ° F difference it will be recorded and the next position taken in

sequence. If more than 0.01°F difference, two percent of the forty first data point (comparator) will be added to the 98 percent of the FTLA, which is now the new FTLA. The forty-second data point will be compared to the new FTLA and if more than 0.10°F , the process will continue until within 0.10°F . Gage positions are sampled in the same way and held to 0.10 ohms. It often takes 20 minutes to take all the hot data. It takes less than five minutes to obtain the zero $^{\circ}\text{F}$ data and less than five minutes for the ambient (78°F) data.

The data was repeatable for both the RTDs and gages but temperature across the circuit boards appear to be non-linear. It was decided that more detailed thermal characterization was necessary to study the degree of non-linearity. Additional insulation near the door of the temperature chamber, the face of the circuit board holder and at the rear of the circuit board holder was added as can be seen in Figure 3.

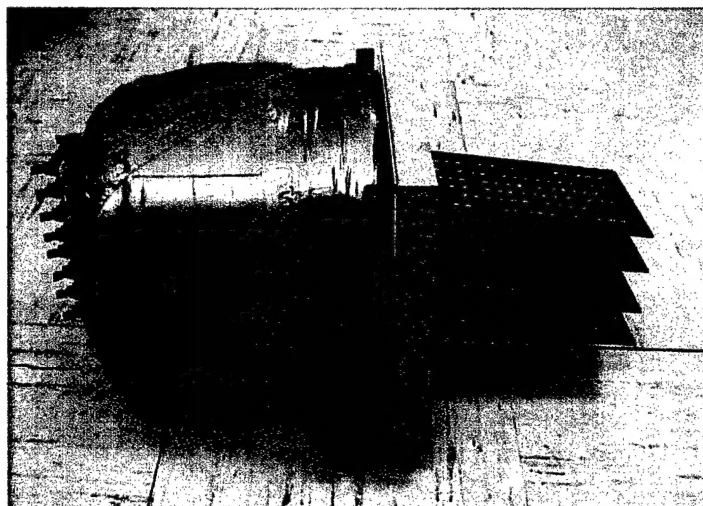


Figure 3. Oven Door Insulation

Analysis from thermal profiling the circuit boards and the temperature profile across the oven showed considerable thermal non-linearity near the door and the worst-case non-linearity was at 278°F and is discussed below. However, the data was repeatable so a correction factor will be added to the straight-line reference. Future refinements will include changes to the circuit board by moving all the gages to the center of the temperature chamber by making the rows shorter and the circuit board wider.

In all cases the current set-up allows the temperature distribution to be calculated with accuracy better than one degree. Recent work has improved and tuned the digital filtering to be faster and more accurate with consistent temperature prediction to within 0.1°F of actual measurements.

1.3 Discussion of Results

Typical results, under the worst conditions, of four previously matched sets of gages from three runs carried out at a nominal 278°F are given in Table A. The actual measured

temperatures on this board was at the rear of chamber (RTDR) 278.14 ± 0.10 ° F, in the middle of the board (RTDM) 280.55 ± 0.45 ° F and at the door end of the board (not shown) 279.56 ± 0.50 ° F. However, the variation across all the boards in the oven is considerably larger with the recorded lowest temperature of 248 ° F and the highest 285 ° F. This board-to-board variation is less than one degree at ambient and only five degrees at the lower temperatures.

| | A | B | C | D | E | F | G |
|------|--------|-----|----|--------|-------|--------|-------|
| 174 | 794.2 | 788 | 8 | 793.81 | 0.39 | 794.51 | -0.7 |
| 175 | 796.28 | 788 | | 796.09 | 0.19 | 796.71 | -0.62 |
| 176 | 792.55 | 788 | | 792.33 | 0.22 | 792.78 | -0.45 |
| 177 | 797.28 | 788 | | 796.87 | 0.41 | 797.22 | -0.35 |
| 178 | 807.81 | 802 | 9 | 807.15 | 0.66 | 807.4 | -0.25 |
| 179 | 807.52 | 802 | | 806.51 | 1.01 | 807.06 | -0.55 |
| 180 | 808.93 | 802 | | 808.12 | 0.81 | 808.33 | -0.21 |
| RTDM | 280.28 | - | | 280.37 | -0.09 | 281 | -0.63 |
| 181 | 831.01 | 802 | | 829.32 | 1.69 | 829.82 | -0.5 |
| 182 | 806.62 | 801 | 10 | 804.25 | 2.37 | 806.29 | -2.04 |
| 183 | 809.16 | 801 | | 807.3 | 1.86 | 809.29 | -1.99 |
| 184 | 812.07 | 801 | | 810.92 | 1.15 | 812.59 | -1.67 |
| RES | 400.35 | - | | 400.44 | -0.09 | 400.41 | 0.03 |
| 186 | 811.68 | 801 | | 810.02 | 1.66 | 810.53 | -0.51 |
| 187 | 811.8 | 808 | 11 | 810.04 | 1.76 | 810.59 | -0.55 |
| 188 | 817.82 | 808 | | 816.53 | 1.29 | 816.96 | -0.43 |
| 189 | 809.23 | 808 | | 808.42 | 0.81 | 808.93 | -0.51 |
| 190 | 807.66 | 808 | | 807.27 | 0.39 | 808.31 | -1.04 |
| RTDR | 278.14 | | | 278.23 | -0.09 | 278.04 | 0.19 |

Table A. Typical Results

The first column is the element position on the board and contains the precision resistor (in this case 400 ohms as it is board four) and the Resistive Temperature Device locations.

The reference number of the matching set of gages tested is shown in column C with the resistance value, measured at 278 ° F using the old system, given in column B.

COLUMN A - The measured resistance of each gage from the first run

COLUMN D - The measured resistance of each gage from the second run

COLUMN F - The measured resistance of each gage from the third run.

Columns E and G are the measured difference in resistance between the runs, which gives an average measurement error of 0.13 ohms with a standard deviation of 1.11 ohms which is repeatable and an order of magnitude improvement on the previous system.

Considering the actual resistance values of the matched sets as shown in column A gives an indication of this improvement:

| | |
|--------|-------------------|
| Set 8 | 795 ± 2 ohms |
| Set 9 | 814 ± 11 ohms |
| Set 10 | 810 ± 3 ohms |
| Set 11 | 812 ± 5 ohms |

Whereas gages matched by the current system will give standard deviations of less than ± 0.2 ohms.

1.4 Conclusions

Sensors fabricated from the gages of set 9, and to a lesser extent set 11 are more likely to result in sensors of reduced thermal stability and increase in long-term drift. Sensors fabricated from gages matched by the new precision system will have an order of magnitude improvement in performance and should have lower cost of manufacture as less effort would be required to calibrate the finished units.

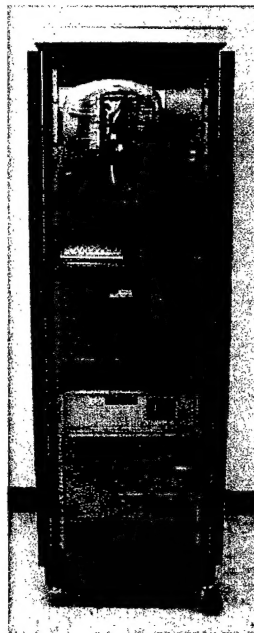


Figure 4. Precision Gage Matching System

The precision gage matching system shown in Figure 4 will permit production of sensors with minimum long-term drift. The uncertainty in the temperature distribution of the old system has been eliminated. Recent work has improved and tuned the digital filtering to be faster and more accurate with consistent temperature prediction to within 0.1°F of actual measurements.

Well designed motors using established propellants with well know characteristics and which are not pushing the technology are expected to last 15 years or more. The error due to long term drift of health monitoring sensors must be within the allowable error band, which could be as low as one psi for such motors. If the drift is low and predictable, the data can be corrected and the accuracy required achieved.

SECTION 2 – Long Term Measurement Stability

Calibration checks of the sensor after casting of the propellant grain is not possible, therefore it is essential that the units used for long term health monitoring are accurate and stable. Any sensitivity change or zero shifts in the sensor output would be indistinguishable from changes in the measured bond stress. Long term changes in balance with no sensor stress have also been run and were found to be acceptable. To test the stress stability of the current system a cantilever constant load test consisting of a static load applied to the sensor diaphragm was initiated and ran for 55 weeks before the bond broke. The stress was applied to the sensor via a hard rubber interface and hanging weights. Extra care was used to ensure that the bonded surface area was limited to be that of the active surface area of the sensor diaphragm. The test rig was exposed to the ambient temperature variations and the data downloaded at regular intervals. The loading fixture is shown in Figure 5 and a local view of the sensor under tension load shown in Figure 6.

An outline of the results for the test is given below with the start and end values for each download period.

| <u>Date</u> | <u>Start(V)</u> | <u>Finish (V)</u> |
|--|-----------------|-------------------|
| 21 st Dec to 31 st Dec | 2.432/1.296 | 2.395/1.598 |
| 31 st Dec to 22 nd Jan | 2.395/1.616 | 2.416/1.703 |
| 22 nd Jan to 19 th Feb | 2.417/1.721 | 2.415/1.720 |
| 20 th Feb to 24 th April | 2.411/1.717 | 2.435/1.725 |
| 2 nd May to 16 th July | 2.437/1.735 | 2.445/1.833 |
| 17 th July to 7 th Dec | 2.456/1.854 | 2.534/1.743 |
| 7 th Dec to 9 th Jan | 2.527/1.705 | 2.926**/1.719 |

** Peak value just before final bond failure.

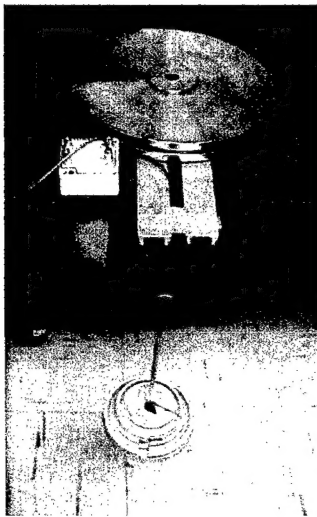


Figure 5. Test Rig

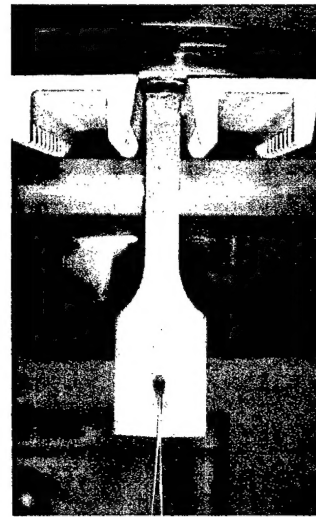


Figure 6. Sensor under Test

The first hour of the loading sequence on the 21st December 2001 is shown in Figure 7 in logger output of volts and a scan rate of five seconds.

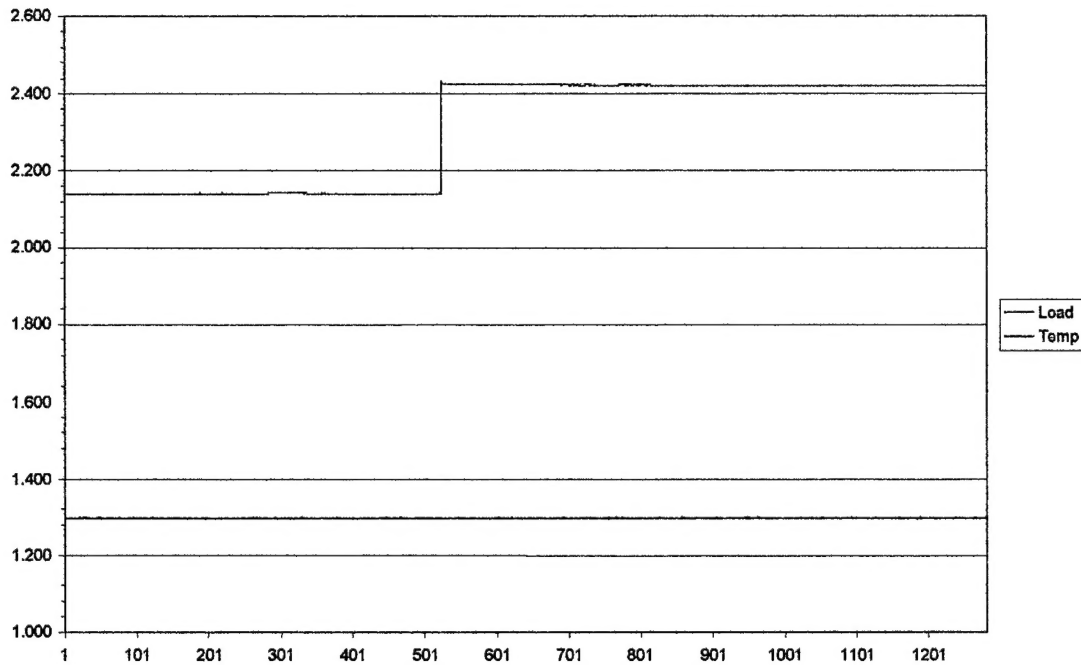


Figure 7. Loading Sequence

The plot of the results for the next twelve months are given in Figure 8 in engineering units which shows that the variation of output is 75 psi to 78 psi for the load, together with the ambient temperature variations. The trend of the load follows the average increase in the ambient temperature until towards the end when there is a significant increase. It is assumed this is due to progressive bond failure at the sensor/rubber interface. Inspection of the bond line gave signs that the edge of the interface around the sensor was separating. This was confirmed because during the last few weeks of sensor output, as given in Figure 9, it can be seen that the load increases as the bond area decreases at an increasing rate until final failure. The recorded peak load as shown in Figure 10 was over 200 psi. With the scan rate of one hour the actual peak value may have been missed and larger. A picture of the bonded area of the sample and shim is given in Figure 11.

The sensors zero value after a temperature correction had increased by 3.8 psi due to creep in the bonds of the semiconductor gages which is considered acceptable after over a year under load at ambient temperature. The sensitivity value, the more important characteristic for long-term stability, showed a change of level less than 0.1% well inside the initial values measured over the temperature range.

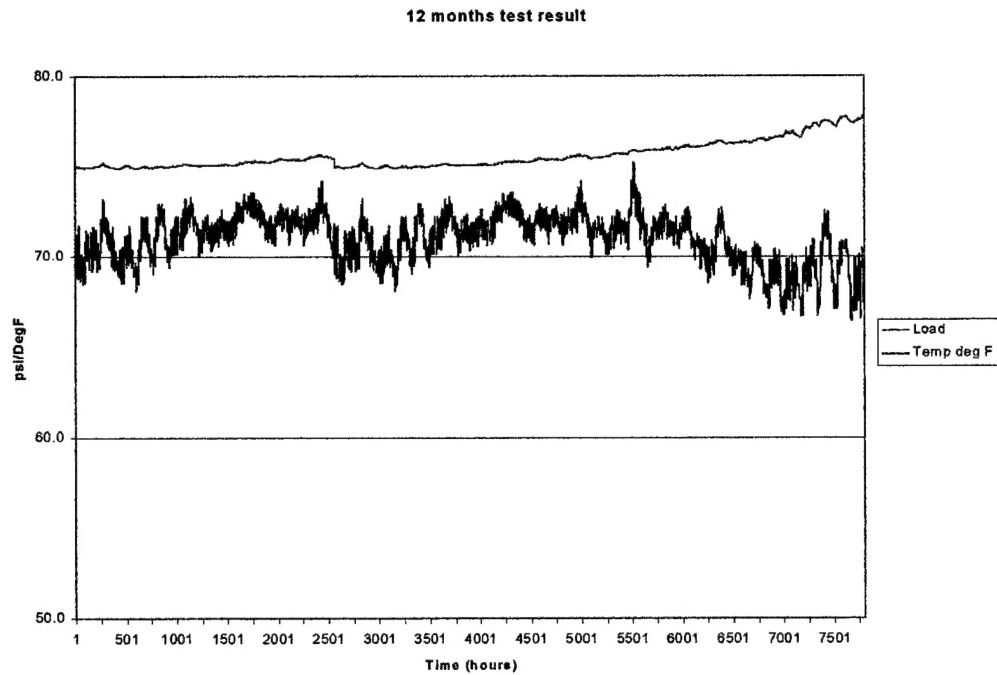


Figure 8. Long Term Stability Test results

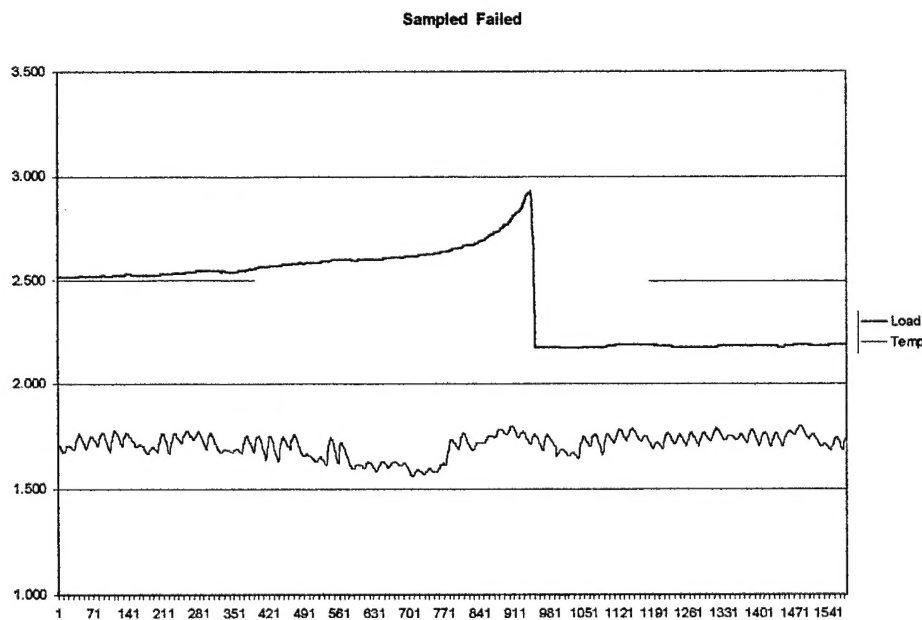


Figure 9. End of Test Bond Failure

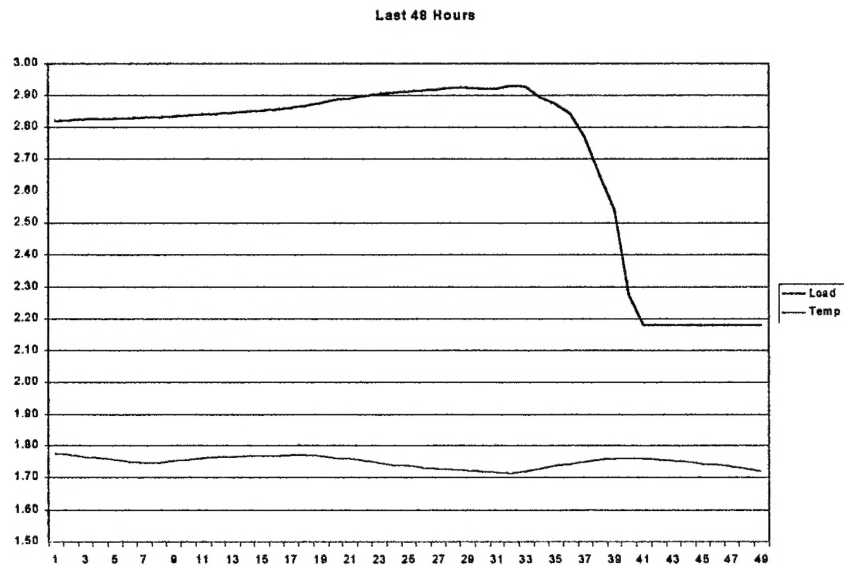


Figure 10. Last Two Days of Test



Figure 11. Failed Sample

SECTION 3 – Conclusions and Recommendations

The precision gage matching system will permit production of sensors with minimum long-term drift. Conservatively designed motors using established propellants with known characteristics and which are not pushing the technology are expected to last 15 years or more. The error due to long term drift of health monitoring sensors must be within the allowable error band, which could be as low as one psi over the life of such motors. If the drift is low and predictable, the data can be corrected and the accuracy required achieved during long term monitoring. The new units should also have lower cost of manufacture, as less effort would be required to temperature compensate the final units.

Results from the constant load test indicate that the current build standard of sensor is stable and shows little creep when under 75% full-scale tensile load for over a year at ambient temperature. The sample broke at the bond line after 55 weeks and the sensor zero had changed by only 3.8 psi with no change in the sensitivity.

Bondline stress data, continuously monitored, may be directly input into cumulative damage-based failure predictive models or may be used as an instantaneous detector of propellant grain cracks and/or debonds. Optimized placement of stress transducers may even allow triangulation to locate an induced flaw. These features have great benefit and great potential to achieve the ultimate goal of health monitoring in solid rocket motors.

The results of design, calibration studies, and functional testing under SBIR contracts provide the Army with confidence that embedded sensors, which accurately interrogate and validate structural integrity for rocket motors can be developed and employed with good precision. SBIR Phase II program objectives have been conceived and are being pursued. Of particular interest is to establish installation procedures and combustion chamber egress designs which can be implemented in a rocket motor production environment, to demonstrate these on a production Army motor design, and support data interface and download with prototype RRAPDS hardware. A sensor package to monitor the loads imposed on the motor during transportation will also be developed and tested.